Photoeffects on the Reduction of Carbon Tetrachloride by Zero-Valent Iron

Barbara A. Balko*

Department of Chemistry, Lewis & Clark College, 0615 SW Palatine Hill Road, Portland, Oregon 97219

Paul G. Tratnyek

Department of Environmental Science and Engineering, Oregon Graduate Institute of Science and Technology, P.O. Box 91000, Portland, Oregon 97291-1000

Received: September 25, 1997

While reduction of chlorinated hydrocarbons by zero-valent iron in water is strongly influenced by the oxide layer at the metal−water interface, the role of the oxide in the dechlorination mechanism has not been fully characterized. In this paper, we investigate the semiconducting properties of the oxide layer on granular iron and show how the electronic properties of the oxide affect electron transfer to aqueous CCl_4. Specifically, we determine whether conduction-band electrons contribute to the reduction of CCl_4 by using light to increase the number of conduction-band electrons at the oxide surface and measuring how this treatment affects the rate and products of CCl_4 degradation. We find that photogenerated conduction-band electrons do degrade CCl_4 and, more importantly, shift the product distribution to more completely dechlorinated products that are indicative of two-electron transfer with a dichlorocarbene intermediate. Since the photogenerated electrons give different reduction products than the dark reducers, we conclude that the latter must not be conduction-band electrons. Further investigation of the reduction with photogenerated electrons is carried out by adding hole scavengers to the system. Isopropyl alcohol reacts with photogenerated holes to yield the α-hydroxyalkyl radical, which is known to reduce CCl_4. With isopropyl alcohol present, we observe faster degradation of CCl_4 with higher light intensity. Since no such increase is seen without isopropyl alcohol, the rate of CCl_4 degradation by conduction-band electrons in water must not be limited by the number of photogenerated electron−hole pairs but rather by electron transfer from the oxide conduction band to CCl_4.

Introduction

Zero-valent iron is currently being used to remediate dilute, aqueous, halogenated hydrocarbon contaminants in ground water.[1] This process is a large-scale, environmental application of a dissolving metal reduction,[2,3] where the oxidation of Fe^0 ($E^0_{red} = -0.44$ V[4])

$$Fe^0 \rightleftharpoons Fe^{2+} + 2e^- \quad (1)$$

drives the reduction of halogenated methanes, ethanes, ethenes, and propanes. In this paper, we investigate the role that the semiconducting properties of iron oxides play in these remediation reactions, specifically degradation of CCl_4. CCl_4 was chosen as our probe compound because it is the most widely used model compound for studying degradation by zero-valent iron, and detailed studies have been carried out on photoreduction of CCl_4 using a colloidal semiconductor (TiO_2).[5,6]

There are two main reaction pathways for the anaerobic reduction of CCl_4: hydrogenolysis (one-electron transfer) and reductive elimination (two-electron transfer).[7−9] Both of these pathways are initiated by dissociative electron transfer[10]

$$CCl_4 + e^- \rightarrow \cdot CCl_3 + Cl \quad (2)$$

to give trichloromethyl radical and chloride ion. In hydrogenolysis, the $\cdot CCl_3$ is reduced to chloroform

$$\cdot CCl_3 + e^- + H^+ \rightarrow HCCl_3 \quad (3)$$

which may undergo further hydrogenolysis to give dichloromethane. The rate of chloroform reduction, however, is much less than the rate of hydrogenolysis of CCl_4.[7,11] In reductive elimination, the $\cdot CCl_3$ undergoes a second dissociative electron transfer to form dichlorocarbene

$$\cdot CCl_3 + e^- \rightarrow :CCl_2 + Cl^- \quad (4)$$

which is hydrolyzed to give HCl and CO.[12,13]

$$:CCl_2 + H_2O \rightarrow CO + 2HCl \quad (5)$$

The net two-electron transfer to form $:CCl_2$ from CCl_4, i.e., reductive elimination

$$CCl_4 + 2e^- \rightarrow :CCl_2 + 2Cl^- \quad (6)$$

is thermodynamically favored over one-electron reduction (reaction 2) and is spontaneous as long as the electron donor has an $E^{0\prime} < \sim 0.2$ V.[9,14] From a remediation standpoint, reductive elimination is preferred over hydrogenolysis because the final products in the former pathway are more environmentally benign.

The immediate source of the electrons that are transferred to CCl_4 is difficult to determine due to the complex chemistry of the interfacial region between iron and water. In principle, reduction might occur by electron transfer directly from Fe^0 or

* Corresponding author. Email: balko@lclark.edu.

S1089-5647(97)03113-1 CCC: $15.00
Published on Web 02/03/1998

from either of the products formed during anaerobic corrosion of the metal (Fe^{2+} or H_2).[7]

$$Fe^0 + H_2O \rightarrow Fe^{2+} + H_2 + 2OH^- \quad (7)$$

Electron transfer from Fe^0 to the aqueous CCl_4 may occur directly from the metal or indirectly through the oxide film. Direct electron transfer between the metal and the organic could occur by tunneling (direct or resonance)[15−19] or through defects such as pits or pinholes that allow the solution to directly contact the iron.[15,20,21] For indirect electron transfer through the oxide film to be significant, there must be a facile mechanism for transporting electrons across the oxide layer, presumably through the conduction band. Exploring the role of conduction-band electrons in reduction of organic adsorbants is the primary objective of this study.

The mechanism of electron transport through the oxide layer (or passive film) will depend, in part, on the composition of this material. There is general agreement that the typical passive film on Fe^0 is composed of Fe_3O_4 (magnetite), which is a mixed-valent, highly conductive oxide,[22−26] and γ-Fe_2O_3 (maghemite), which is an n-type semiconductor.[22,23,27−31] The arrangement of these oxides in the passive film is undoubtedly variable but is thought to conform to one of two models.[30] In one model, the film has an inner layer of Fe_3O_4 and an outer layer of γ-Fe_2O_3.[23,27−30] Alternatively, the film may have a continuous Fe^{2+} concentration gradient, with the concentration equal to that found in Fe_3O_4 at the oxide−iron interface and decreasing to that of γ-Fe_2O_3 at the oxide−solution interface.[22,30,31]

Raman studies suggest that the air-formed oxide film present on the granular iron used in our studies is similar in composition to the passive film.[32] These studies show that the outer layer of the air-formed film is primarily comprised of γ-Fe_2O_3 with some α-Fe_2O_3 present (the percentage depends on the original composition and subsequent handling of the iron particles) while the inner layer is Fe_3O_4. Exposure of the iron particles for several weeks to ground water contaminated with chlorinated solvents results in disappearance of the Fe_2O_3, presumably due to autoreduction of the Fe(III) oxide to Fe_3O_4 and formation of green rust.[32] However, since our experiments were completed within 3 h, our films presumably will retain the composition of the original air-formed oxide.

Under illumination, the typical passive film behaves like an n-type semiconductor with a band gap of ∼1.9 eV, a flatband potential of −0.3−0.0 V (vs NHE at pH 7), and a doping density of $\sim 10^{20}$ cm^{-3}.[33−36] The passive film on Fe^0 has been successfully modeled as semiconducting Fe_2O_3 that is highly doped (5×10^{20} cm^{-3}) with Fe^{2+}.[37] (However, if the passive film has a continuous Fe^{2+} concentration gradient, the doping density cannot be uniform through the thickness of the film.[35]) Electron energy levels for the iron/oxide/aqueous CCl_4 system compiled from previously published values[14,34−36,38−45] are summarized in Figure 1. The energy levels of the oxide are from photoelectrochemical experiments in which the film was treated as a one-component, single-crystal semiconductor so the oxide layer is drawn as such.

Figure 1 reveals several constraints on electron transfer through the oxide film. First, the Fermi energy (E_F) of the iron oxide is more negative than that of the iron metal, so once equilibrium is established there will be a potential barrier for injecting electrons from the iron metal to the conduction band of the iron oxide.[42] Second, $E^0(CCl_4/{\cdot}CCl_3, Cl^-)$ is more positive than the conduction-band energy, which means that the unoccupied electron energy levels of the redox couple can overlap with the conduction band. The likelihood of electron transfer

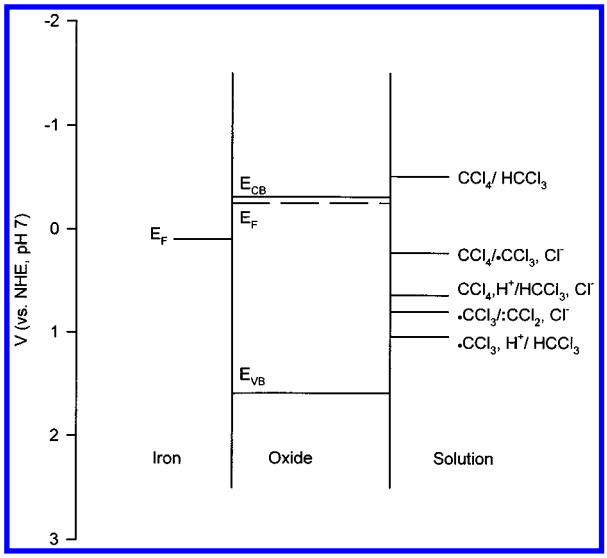

Figure 1. Band diagram of the iron/oxide/aqueous CCl_4 system at pH 7, constructed using electron energies versus the normal hydrogen electrode (NHE) from the literature. The diagram shows (i) The Fermi energies, E_F, for Fe^0 (calculated from the work function[42]) and the oxide layer (literature values cluster between −0.18[35] and −0.33 V;[34] the average, −0.25 V, is used in the diagram); (ii) the lower edge of the oxide conduction band, E_{CB}, ($E_F - E_{CB} = \sim 0.06$ eV, assuming an effective density of energy levels at the conduction band edge of $\sim 10^{19}$ cm^{-3} [41] and a doping density of 10^{20} cm^{-3};[34,36,39] (iii) the upper edge of the oxide valence band, E_{VB}, calculated from the value of E_{CB} and assuming a band gap of 1.9 eV;[34,36,38] (iv) the E^0's for relevant redox couples: $CCl_4 + e^- \rightarrow {\cdot}CCl_3 + Cl^-$,[14] ${\cdot}CCl_3 + H^+ + e^- \rightarrow HCCl_3$,[14] $CCl_4 + H^+ + 2e^- \rightarrow HCCl_3 + Cl^-$,[14] $CCl_4 + H^+ + 2e^- \rightarrow CHCl_3 + Cl^-$,[40] and ${\cdot}CCl_3 + e^- \rightarrow :CCl_2 + Cl^-$ (calculated using the method outlined in ref 45 with thermodynamic values from refs 43 and 44) and assuming $[Cl^-] = 10^{-3}$ M).

from a semiconductor to the electrolyte is greater if there is good overlap between the conduction-band edge and the unoccupied electron energy levels of the redox couple.[15,46] Third, because E_F of the oxide is more negative than $E^0(CCl_4/{\cdot}CCl_3, Cl^-)$, the oxide film may be in depletion; i.e., there may be a space charge region in the oxide film that acts as a barrier to electron transport from the conduction band to the solution. It should be noted that this barrier arises as equilibrium is established between the semiconductor and the redox couple in solution, and that electron transfer occurs from the semiconductor to solution until $E^0(\text{oxide}) = E_F(\text{redox})$.[41] This barrier may not be fully established, however, because the rate at which equilibration occurs depends on the rate of charge transfer between the oxide and the redox couple,[41] and this is likely to be slow for the iron/oxide/aqueous CCl_4 system.[11,47]

The details of the electronic structure of the passive film differ from that of the single-crystal semiconductor portrayed in Figure 1, primarily because passive films lack long-range order. Passive films are typically only a few monolayers thick, so long-range order normal to the surface cannot develop. Thicker films tend to be amorphous because a more coherent film would be strained and break up.[15,17,18,38,48] While the electronic structure will vary with film thickness and the conditions under which the film is grown (potential, electrolyte, etc.), several generalizations can be made regarding the air-formed oxide film involved in this study. First, while the film will have bands equivalent to the conduction and valence bands found in single-crystal semiconductors, additional bands, which result from a large density of impurities or ions in a different oxidation state, may also be found.[15,22] In addition, there will be a much greater density of localized states than found in single-crystal semi-

conductors. These localized states result from the lack of identical lattice sites throughout the film.[15,17,18,22,38]

Electron transfer between the oxide layer and adsorbed species can occur via the oxide conduction band, impurity bands, or localized states.[15,35,39,49] For example, several studies have shown that electrons are transferred from the conduction band of the passive film on iron to $Fe(CN)_6^{3-}$.[50,51] Yet Fe^{2+} provides localized states, which can facilitate resonance tunneling through iron oxide films.[52] A specific goal of this study was to determine if conduction-band electrons are responsible for the reduction of CCl_4 by iron metal. The approach taken was to manipulate the number of conduction-band electrons that reach the surface of the oxide film by the addition of light.

There are two main mechanisms whereby light can increase the number of conduction-band electrons at the oxide−water interface. First, assuming that the oxide film is in depletion, photogenerated electrons and holes cause the bands to flatten, thereby reducing the barrier for tunneling of conduction-band electrons through the space charge region to the oxide surface.[41,53] The second effect that the light may have is generation of conduction-band electrons in the oxide layer. If the contact potential barrier between the iron metal and the oxide layer is large enough to impede electron injection from the iron metal into the oxide layer, then there will be a greater number of conduction-band electrons available at the oxide surface.

In the experiments described below, batch studies were done with CCl_4 and zero-valent iron in the presence and absence of light with energy greater than the oxide layer band gap. The results show that while photogenerated conduction-band electrons are formed on iron particles and contribute to the degradation of CCl_4, conduction-band electrons are not responsible for the dechlorination of CCl_4 by Fe^0 in the dark.

Experimental Section

In the typical batch experiment, vials were filled under an N_2/H_2 atmosphere with 12 mL of deoxygenated/deionized water, 1.0 g of 20−32 mesh Fe^0 turnings (Fluka, puriss. grade, specific surface area = 0.019 $m^2\ g^{-1}$), and CCl_4 at an initial concentration of 85 μM. The vials were crimp-sealed without headspace and rotated at 30 rpm. Periodically, vials were sacrificed and aqueous samples extracted with hexane. The extract was then analyzed by gas chromatography with electron-capture detection. In experiments where 0.1 M isopropyl alcohol was used, the concentration of acetone formed was monitored by derivatization with 2,4-dinitrophenylhydrazine and analysis of the product by high-performance liquid chromatography.[54] First-order kinetics for the disappearance of CCl_4 was observed, as expected, and rate constants were obtained by linear regression of $\ln[CCl_4]$ versus time data. Reported uncertainties are 1 standard deviation about the regression line.[11]

To create conduction-band electrons, it was necessary to supply light with energy greater than the band gap of the oxide film. Photocurrent has been detected from an iron passive film in borate buffer with light up to ~730 nm, with the peak photocurrent occurring at ~400 nm.[38] The wavelength maximum, however, undoubtedly depends on the conditions under which the film was grown. To ensure that the photons supplied have sufficient energy, we chose to use a 1000-W solar simulator (Oriel #81193), which emits light from ~250 to ~2500 nm. Since the solar simulator has a 6 × 6 in. beam, this had the added advantage of allowing us to illuminate all vials simultaneously. For most of the experiments, we used an Air Mass 0 (AM0) filter (Oriel #81011) which corrects the xenon arc lamp output to match the solar spectrum outside the earth's atmosphere. We estimated the power supplied to be 720 W/m^2 in the 280−700-nm range and 170 W/m^2 in the 320−450-nm range, based on data supplied by Oriel. The projected area of the iron particles in the vials was ~3 cm^2. In some experiments, the intensity of the solar simulator was decreased by inserting an Air Mass 1 (AM1) filter (Oriel #81074), which gives an output equivalent to the solar spectrum at ground level. With this filter installed, we estimated the output power to be 575 W/m^2 in the 280−700-nm range and 115 W/m^2 in the 320−450-nm range.

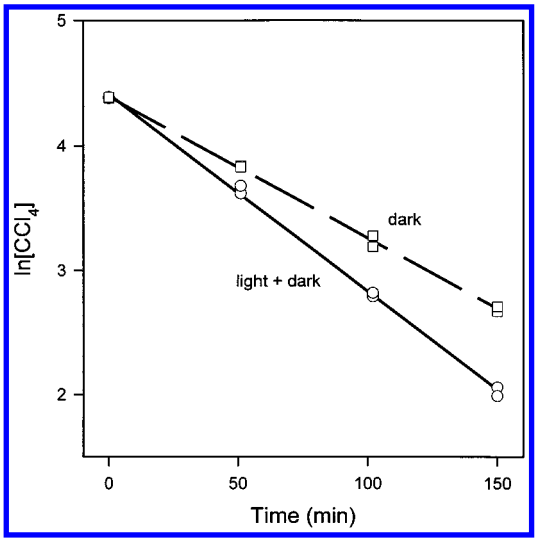

Figure 2. Typical kinetics of CCl_4 degradation by Fe^0 with and without the addition of light (AM0). Squares and circles are for experiments run in the dark and light, respectively. The lines show the best fit to a first-order kinetics model.

In all experiments, we included dark controls by wrapping vials in aluminum foil and adding them to the rotator. The degradation rates obtained in the light (k_{L+D}) represent the sum of the rate of CCl_4 degradation in the dark (k_D) and CCl_4 degradation due to the addition of light (k_L). To quantify the rate of degradation due to the light alone, the rate constant for dark degradation was subtracted from that measured in the light (i.e., $k_L = k_{L+D} - k_D$). Direct homogeneous photolysis should be negligible since CCl_4 has very little absorbance at wavelengths greater than 270 nm,[55] the borosilicate glass vials used transmit little light below 290 nm,[56] and the solar simulator puts out only a small percentage of its power at wavelengths below 320 nm (0.8% for AM0 and 0.2% for AM1). However, because the effect of light on CCl_4 degradation was also small, we felt it was important to quantify the rates of homogeneous CCl_4 photolysis due to the addition of light ($k_{no\ Fe,L}$) as well as CCl_4 loss in the dark in the absence of iron ($k_{no\ Fe,D}$), which is likely due to processes such as adsorption on the septa, volatilization, and hydrolysis. We found $k_{no\ Fe,D} = 0.07 \pm 0.01\ h^{-1}$ and $k_{no\ Fe,L} = 0.07 \pm 0.02\ h^{-1}$. These were subtracted from the measured rates of CCl_4 degradation in the presence of iron ($k_{meas,D}$ and $k_{meas,L+D}$) for all the kinetic data reported below (i.e., $k_D = k_{meas,D} - k_{no\ Fe,D}$ and $k_{L+D} = k_{meas,L+D} - k_{no\ Fe,L} - k_{no\ Fe,D}$).

Results and Discussion

Effect of Light on the Rate of CCl_4 Degradation. *In Water.* The addition of light to batch systems of iron and water consistently increased the rate of CCl_4 degradation; this increase in rate shows that conduction-band electrons do indeed reduce aqueous CCl_4. Figure 2 shows typical kinetics for the degradation of CCl_4 with and without the addition of light. In this

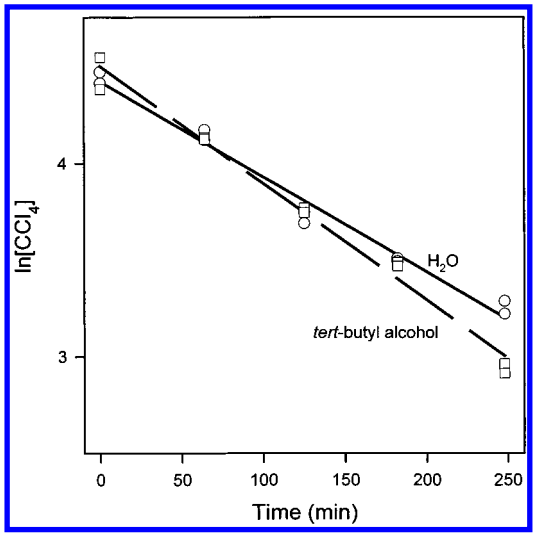

Figure 3. Effect that the addition of 0.1 M *tert*-butyl alcohol has on CCl_4 degradation by Fe^0 in the light (natural sunlight). Squares are for 0.1 M *tert*-butyl alcohol and circles are for deionized water. The lines show the best fit to a first-order kinetics model.

example, $k_L = 0.20 \pm 0.05\ h^{-1}$ and $k_D = 0.68 \pm 0.01\ h^{-1}$, so the degradation rate due to photogenerated electrons is approximately one-third of the rate observed in the dark (based on $k_L/k_D = 0.33 \pm 0.1$). The photoeffect, the increase in the rate of CCl_4 degradation due to the addition of light to the experiment, may be small because degradation is slower when photogenerated electrons are responsible for reduction or because fewer photogenerated electrons are available than dark reducers. (By dark reducers we mean the species responsible for reduction in the dark, whether it be surface Fe(II), electrons that are transferred directly from the iron via tunneling or defects, or electrons that are transported through the conduction band of the oxide film.) It is not known, however, how many conduction-band electrons are produced for each photon supplied, or the number of active dark reducers, so it is not yet possible to compare the rates for light and dark degradation on a microscopic level.

In 0.1 M tert-Butyl Alcohol. Although we expected that the photoeffect is due to production of conduction-band electrons, it is also possible that the photoeffect is due to formation of surface Fe(II) sites via ligand-to-metal charge transfer (LMCT). Light may drive LMCT between adsorbed hydroxide ions and excited surface Fe(III) lattice atoms[57,58]

$$\equiv Fe(III)-OH^- + h\nu \rightarrow \equiv Fe(III)^*-OH^- \rightarrow \equiv Fe(II) + {}^{\cdot}OH \quad (8)$$

Studies on the photochemistry of aqueous Fe(III), however, show that the yield of aqueous Fe(II) due to the LMCT mechanism is quite small in the absence of ·OH scavengers [quantum yield $\sim 10^{-4}$ [58]]. It is unlikely, then, that LMCT is responsible for our photoeffect. Moreover, addition of the ·OH scavenger *tert*-butyl alcohol, which should increase the yield of Fe(II) via the LMCT mechanism,[58] did not lead to a significant increase in the rate of CCl_4 degradation in the presence of light (Figure 3). Thus, we conclude that the increase in degradation rate that occurs with the addition of light is not due to the formation of Fe(II) sites via LMCT but is due to the creation of conduction-band electrons.

Effect of Light on the Distribution of CCl_4 Degradation Products. Comparison of the product distributions obtained from CCl_4 degradation in the light and the dark suggests that

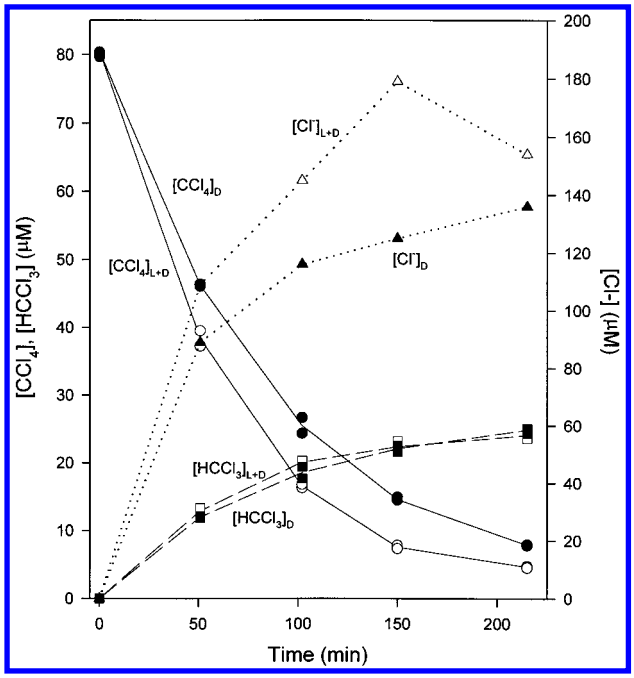

Figure 4. Effect of light on major products of CCl_4 degradation by Fe^0. Concentrations of CCl_4 (circles/solid lines), $HCCl_3$ (squares/dashed lines), and Cl^- (triangles/dotted lines) were measured in the dark (D, filled symbols) and in the light (L+D, open symbols). The lines connect average concentrations.

degradation by photogenerated electrons follows a different reaction pathway than that involving the dark reducers. As shown in Figure 4, the addition of light did not increase the amount of chloroform formed, even though the rate of CCl_4 degradation and Cl^- accumulation both increase. Reduction of $HCCl_3$ by iron is much slower than reduction of CCl_4 in the dark ($k_{SA} \approx 10^{-3}$ L m^{-2} h^{-1} for $HCCl_3$ versus $\approx 10^{-1}$ L m^{-2} h^{-1} for CCl_4[11] where k_{SA} is the first-order degradation rate constant adjusted for surface area) as well as in the light (data not shown). Therefore, it is likely that the more complete dechlorination observed in the presence of light is due to two-electron transfer to give dichlorocarbene, which then undergoes hydrolysis to give HCl and CO (according to reaction 5), rather than further reduction of chloroform. The change in product distribution that occurs with the addition of light cannot be due to direct, homogeneous photolysis for two reasons. First, direct photolysis of CCl_4 in aqueous solution is quite slow, as evidenced by the fact that there is no significant production of Cl^- during control experiments without iron. Second, the homogeneous photolysis pathway most likely involves only the production of ·CCl_3, which would lead to $HCCl_3$.

Previous reports have shown that the two-electron-transfer pathway is favored when the potential of the reducer is made more negative. For example, Pt deposits, which are known to shift the Fermi energy level in TiO_2 to more negative potentials,[59] increase the amount of two-electron-transfer relative to one-electron transfer in the photoreduction of halothane by *n*-TiO_2.[60] While the second electron transfer step is thermodynamically more favorable than the first step, the Pt deposits are necessary to ensure efficient two-electron transfer as there are many other species present that compete with the photogenerated conduction-band electrons for the intermediate radical, ·$CHClCF_3$. Further evidence that a more negative potential favors two electron transfer can be found in the photodegradation of CCl_4 using *n*-TiO_2 particles, where high pH was found to strongly favor two-electron transfer via dichlorocarbene. While part of the explanation for this pH effect is that hydrolysis of

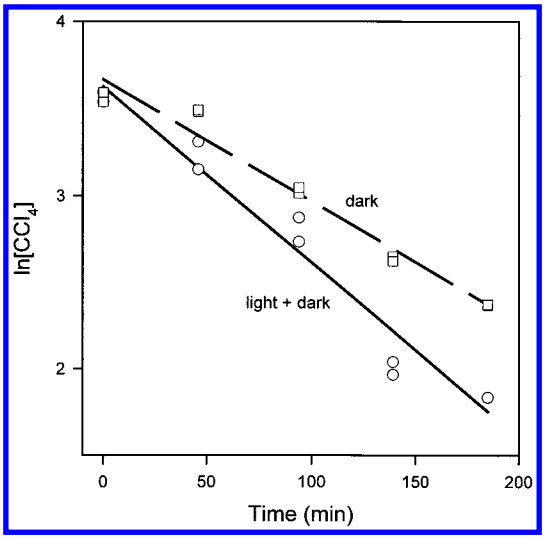

Figure 5. Typical kinetics showing the effect of lower intensity light (AM1). The squares and circles are data from experiments run in the dark and light, respectively. The lines show the best fit to a first-order kinetics model.

$:CCl_2$ to form CO and HCl is base-catalyzed, the Nernstian shift in the conduction band electron reduction potential that occurs with higher pH is also important because it favors electron transfer.[5,6]

The change in distribution of products that occurs with the addition of light implies that the degradation mechanisms involving photogenerated electrons and dark reducers are different. Thus, the dark reducers cannot be conduction-band electrons but must be either electrons transferred directly from the iron or surface Fe(II). In principle, comparison of the reduction potential of the two possible dark reducers with the reduction potential of conduction-band electrons (−0.3 V) allows us to determine which is likely to be more important (recall Figure 1). Electrons transferred directly from the iron are a good candidate for the dark reducer because they are at the Fermi energy of the metal, which has a more positive reduction potential than the photogenerated electrons. The reduction potential for aqueous Fe^{2+}/Fe^{3+} is 0.77 V,[61] but the reduction potential of Fe(II) complexes are considerably more negative: for example, E^0 at pH 7 for Fe^{2+}/α-Fe_2O_3(s) is −0.28 V and for Fe_2SiO_4(s)/Fe_3O_4(s) is −0.43 V.[62] Until the reduction potential of Fe(II) sites in the oxide can be determined, the role of surface Fe(II) sites in the dark reaction cannot be fully resolved from this study.

Effect of Light Intensity on CCl_4 Degradation. *In Water.* Since conduction-band electrons appear to be responsible for reduction of CCl_4 in the light, we expected that the rate of degradation would vary with the irradiation intensity. Figure 5 shows the kinetics of CCl_4 degradation at the low light intensity (AM1). Comparison of rate constants obtained from this experiment with those obtained under high light intensity (AM0), shows that light intensity does not have a significant effect on the ratio k_L/k_D (Table 1). One possible explanation for the apparent lack of an intensity effect is that the reaction of conduction-band electrons with CCl_4 is slow relative to other reactions involving these reducers. For example, the photogenerated conduction-band electrons may react predominantly with trapped holes, reduce Fe(III) lattice sites,[63] or reduce H_2O to H_2. It is also possible that the effect of light intensity is not detectable because the range of light intensity used is too narrow; e.g., production of electron−hole pairs may be saturated at low light intensities because the oxide film is not a strong absorber.

TABLE 1: Light Intensity Effects on CCl_4 Degradation in Water

	k_L/h^{-1}	k_D/h^{-1}	k_L/k_D
AM1	0.12 ± 0.09	0.31 ± 0.04	0.38 ± 0.3
AM0	0.20 ± 0.05	0.61 ± 0.02	0.33 ± 0.1

[a] All rate constants have been corrected for degradation in the absence of iron. In correcting k_L(AM1), we assumed that the homogeneous photolysis rate constant ($k_{no\ Fe,L}$) is the same as with the AM0 filter, making k_L and k_L/k_D upper estimates.

However, results described in the following section indicate that increasing the light intensity in the presence of hole scavengers increases the number of holes produced so it must also increase the number of conduction-band electrons. This leaves us with the conclusion that reaction of conduction-band electrons with CCl_4 is a minor pathway and therefore negligibly effected by modest changes in light intensity.

In 0.1 M Isopropyl Alcohol. Isopropyl alcohol was used to investigate the weak dependence of the CCl_4 reduction rate on light intensity in water. Isopropyl alcohol reacts with photogenerated holes or ·OH (from $h^+ + OH^-$) to generate the α-hydroxyalkyl radical, $(CH_3)_2$(·C)OH, which can reduce CCl_4 to $\cdot CCl_3$.[5,6,64,65] The $\cdot CCl_3$ can then abstract H atoms from the alcohol to give $HCCl_3$.

$$h^+/\cdot OH + (CH_3)_2CHOH \rightarrow (CH_3)_2(\cdot C)OH + H^+/H_2O \quad (9)$$

$$(CH_3)_2(\cdot C)OH + CCl_4 \rightarrow (CH_3)_2CO + H^+ + Cl^- + \cdot CCl_3 \quad (10)$$

$$\cdot CCl_3 + (CH_3)_2CHOH \rightarrow HCCl_3 + (CH_3)_2(\cdot C)OH \quad (11)$$

The product distribution we observed confirms that reduction of CCl_4 via $(CH_3)_2$(·C)OH occurs with the addition of isopropyl alcohol. Figure 6 shows CCl_4, $HCCl_3$, and Cl^- concentrations versus time in the light (AM0) and the dark with isopropyl alcohol present. The observed effect of light on the product distribution differs from that without alcohol (Figure 4) in that there is significantly more $HCCl_3$ formed as a result of H atom abstraction by $\cdot CCl_3$. Acetone was also detected, and Figure 7 shows the concentration of acetone and $HCCl_3$ produced due solely to the addition of light and isopropyl alcohol. Throughout most of the experiment, the amounts of $(CH_3)_2CO$ and $HCCl_3$ produced are approximately equal, as expected if eqs 9−11 apply. Toward the end of the experiment, the concentrations of the two species begin to differ, which may be due to the lower CCl_4 concentration or changes in the oxide layer.

Light intensity has a significant effect on the CCl_4 degradation rate in the presence of isopropyl alcohol. Figure 8 and Table 2 show that this is entirely due to changes in k_L. The effect can be explained by the production of more $h^+/\cdot OH$ pairs with higher intensity light, which leads to a greater number of $(CH_3)_2$-(·C)OH radicals. That we generate more $h^+/\cdot OH$ with the additional light implies that more conduction-band electrons are produced: i.e., we did not saturate the number of electron−hole pairs. It should be noted that the hole-scavenging ability of isopropyl alcohol[5,58] is not responsible for the increase in CCl_4 degradation rate since a depletion region likely exists in the oxide film, which already serves to separate the photogenerated electron−hole pairs. If hole scavenging were critical, addition of *tert*-butyl alcohol would have increased the CCl_4 degradation rate. Thus, since light intensity had no significant effect on the CCl_4 degradation rate in the absence of isopropyl

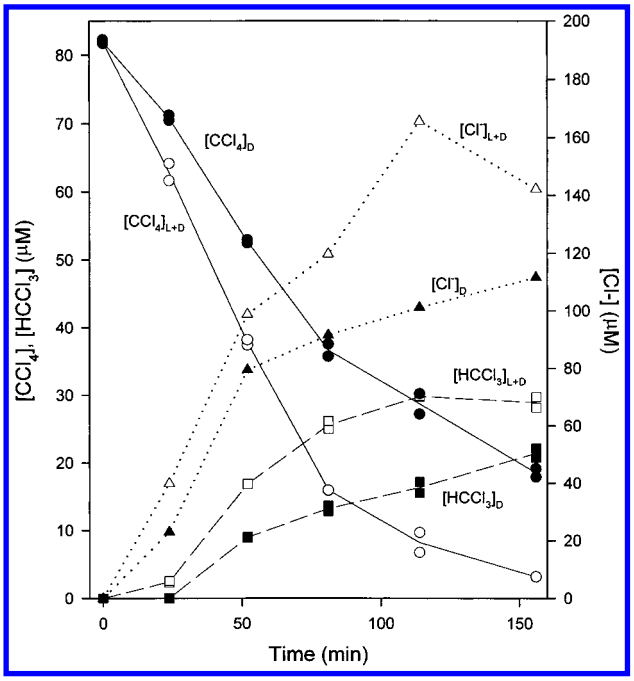

Figure 6. Typical CCl_4 degradation and formation of $HCCl_3$ and Cl^- products showing the effect of light in a batch experiment with the iron/0.1 M isopropyl alcohol/CCl_4 system. The concentrations of CCl_4 (circles/solid lines), $HCCl_3$ (squares/dashed lines), and Cl^- (triangles/dotted lines) were measured in the dark (D, filled symbols) and in the light (L+D, open symbols). The lines connect average concentrations.

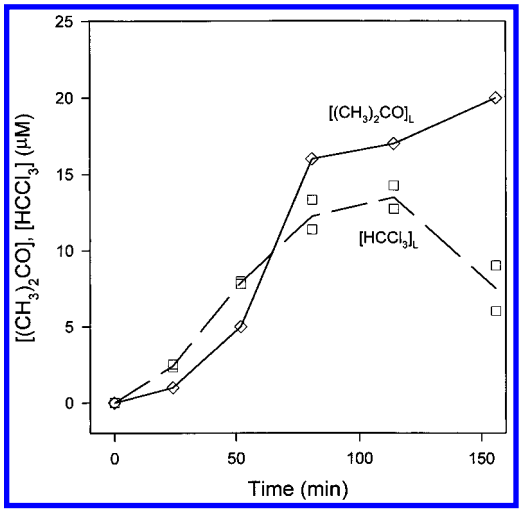

Figure 7. Concentrations of $(CH_3)_2CO$ (triangles/solid line) and $HCCl_3$ (squares/dashed line) produced solely due to the photogenerated electron−hole pairs versus time in batch experiments run in 0.1 M isopropyl alcohol. These concentrations ($[\ ]_L$) were calculated by subtracting the concentrations measured in the dark($[\ ]_D$) from those measured in the light ($[\ ]_{L+D}$). The lines connect average concentrations.

alcohol, reduction of CCl_4 by conduction-band electrons must become "saturated" at high light intensities.

Implications for Environmental Applications

The results of this work narrow the possible mechanisms for how electron transfer occurs in the reduction of CCl_4 by zero-valent iron in the dark. The different product distributions that we observe for CCl_4 degradation in the light and dark suggest that dark reduction does not involve transport of electrons from the iron metal to the CCl_4 via the oxide conduction band. Alternative mechanisms that deserve further investigation include direct electron transfer from the metal to CCl_4 (via

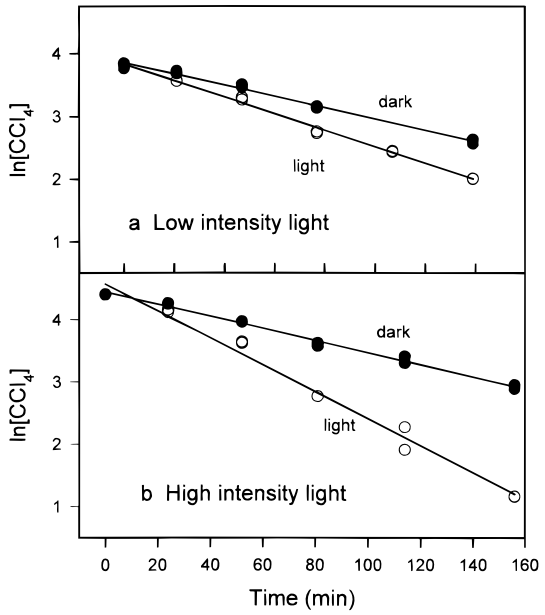

Figure 8. Effect that light intensity has on the CCl_4 degradation rate in iron/0.1 M isopropyl alcohol/CCl_4 systems. In both (a) and (b), the filled circles are data from experiments run in the dark. The open circles show data taken from the experiment run in the light. In (a), AM1 light intensity was used while in (b), AM0 was used. Note that the same axis scale applies to (a) and (b). The solid lines show the best fit assuming first-order kinetics.

TABLE 2: Light Intensity Effects on CCl_4 Degradation in 0.1 M Isopropyl Alcohol

	k_L/h^{-1}	k_D/h^{-1}	k_L/k_D
AM1	0.18 ± 0.06	0.47 ± 0.03	0.38 ± 0.14
AM0	0.64 ± 0.09	0.52 ± 0.02	1.3 ± 0.3

[a] All rate constants have been corrected for degradation in the absence of iron. In correcting k_L(AM1), we assumed that the homogeneous photolysis rate constant ($k_{no\ Fe,L}$) is the same as with the AM0 filter, making k_L and k_L/k_D upper estimates.

tunneling or defects such as pits) and reduction by Fe(II) sites on the oxide surface.

If electron transport across the oxide film via tunneling is how electrons are transferred from the iron to CCl_4, the degradation reaction might be enhanced by increasing conductivity across the layer. The addition of resonance sites into the oxide film by ion-implantation,[66] increasing the Fe^{2+} bulk concentration by passivation of the iron in the light after removal of the air-formed layer,[33,52] or the use of iron alloys may increase the probability of resonance tunneling and, as a result, the rate of electron transfer. Increasing the number of defects in the film, for example, by inducing pitting, may allow direct contact between the iron metal and solution, leading to an increase in the electron-transfer rate. Alternatively, if Fe(II) sites on the oxide surface are responsible for the reduction of CCl_4 in the dark,[67,68] increasing their concentration by adsorption of Fe^{2+} or electron injection by highly reducing species should increase the rate of CCl_4 degradation.

CCl_4 reduction by photogenerated conduction-band electrons leads to greater dechlorination, presumably because the conduction-band electrons have a more negative reduction potential than the dark reducers. Since $HCCl_3$ is an undesirable product in remediation applications, the results of this work suggest that formation of the unwanted product might be minimized by designing the system to favor two-electron transfer: e.g., by lowering the reduction potential of the dark reducer.

The addition of isopropyl alcohol dramatically increased the rate of reduction of CCl_4 by zero-valent iron in the light. This is due to the generation of the α-hydroxyalkyl radical $(CH_3)_2$-(·C)OH, which reduced the CCl_4 to $\cdot CCl_3$. Under these conditions, $HCCl_3$ was a significant product because of H atom abstraction from $(CH_3)_2CHOH$. This result suggests that the presence of H atom donors (including dissolved organic matter or organic buffers) may shift product distribution toward $HCCl_3$, whenever $\cdot CCl_3$ is an intermediate. In this way, secondary components (in laboratory solutions as well as ground water) may affect product distributions to a greater degree than is generally recognized.

Acknowledgment. M. M. Scherer made many helpful contributions to the experimental design and data analysis. D. Romanowski contributed preliminary data as a summer student in the Apprenticeships in Science and Engineering Program. J. Higa and D. Severson made helpful contributions to final experiments as part of the Lewis & Clark College Summer Science Research Program, with support from the Murdock Trust. Acknowledgment is made to the donors of the Petroleum Research Fund, administered by the ACS, for the primary support of this research (29995-AC5).

References and Notes

(1) Tratnyek, P. G. *Chem. Ind.* **1996**, 1 July, 499.
(2) Hudlicky, M. *Reductions in Organic Chemistry*; Halsted: New York, 1984.
(3) House, H. O. In *Modern Synthetic Reactions*, 2nd ed.; Benjamin: Menlo Park, CA, 1972; p 145.
(4) Bratsch, S. G. *J. Phys. Chem. Ref. Data* **1984**, *18*, 1.
(5) Choi, W.; Hoffmann, M. R. *Environ. Sci. Technol.* **1995**, *29*, 1646.
(6) Choi, W.; Hoffmann, M. R. *J. Phys. Chem.* **1996**, *100*, 2161.
(7) Matheson, L. J.; Tratnyek, P. G. *Environ. Sci. Technol.* **1994**, *28*, 2045.
(8) Roberts, A. L.; Totten, L. A.; Arnold, W. A.; Burris, D. R.; Campbell, T. J. *Environ. Sci. Technol.* **1996**, *30*, 2654.
(9) Criddle, C. S.; McCarty, P. L. *Environ. Sci. Technol.* **1991**, *25*, 973.
(10) Savéant, J.-M. In *Advances in Physical Organic Chemistry*; Bethell, D., Ed; Academic: London, 1990; Vol. 26, pp 1.
(11) Johnson, T. L.; Scherer, M. M.; Tratnyek, P. G. *Environ. Sci. Technol.* **1996**, *30*, 2634.
(12) Pliego, J. R., Jr.; De Almeida, W. B. *J. Phys. Chem.* **1996**, *100*, 12410.
(13) Robinson, E. A. *J. Chem. Soc.* **1961**, 1663.
(14) Totten, L. A.; Roberts, A. L. *Division of Environmental Chemistry, Preprints of Papers*; 209th American Chemical Society National Meeting. Anaheim, CA, 1995; Vol. 35, p 702.
(15) Morrison, S. R. *Electrochemistry at Semiconductor and Oxidized Metal Electrodes*; Plenum: New York, 1980.
(16) Schmickler, W. *J. Electroanal. Chem.* **1977**, *82*, 65.
(17) Stimming, U. *Langmuir* **1987**, *3*, 423.
(18) Newmark, A. R.; Stimming, U. *Electrochim. Acta* **1987**, *32*, 1217.
(19) Leiva, E.; Meyer, P.; Schmickler, W. *Corros. Sci.* **1989**, *29*, 225.
(20) Miller, C.; Cuendet, P.; Grätzel, M. *J. Phys. Chem.* **1991**, *95*, 877.
(21) Gu, Y.; Waldeck, D. H. *J. Phys. Chem.* **1996**, *100*, 9573.
(22) Gerischer, H. *Corros. Sci.* **1989**, *29*, 191.
(23) Stimming, U.; Schultze, J. W. *Electrochim. Acta* **1979**, *24*, 858.
(24) Castro, P. A.; R.Vago, E.; Calvo, E. J. *J. Chem. Soc., Faraday Trans.* **1996**, *92*, 3371.
(25) Cox, P. A. *Transition Metal Oxides: An Introduction to their Electronic Structure and Properties*; Oxford: New York, 1995.
(26) Anderman, M.; Kennedy, J. H. In *Semiconductor electrodes*; Finklea, H. O., Ed; Elsevier: New York, 1988; pp 147.
(27) Davenport, A. J.; Sansone, M. *J. Electrochem. Soc.* **1995**, *142*, 725.
(28) Bockris, J. O. M. *Corros. Sci.* **1989**, *29*, 291.
(29) Ryan, M. P.; Newman, R. C.; Thompson, G. E. *J. Electrochem. Soc.* **1995**, *142*, L177.
(30) Oblonsky, L. J.; Davenport, A. J.; Ryan, M. P.; Isaacs, H. S.; Newman, R. C. *J. Electrochem. Soc.* **1997**, *144*, 2398.
(31) Cahan, B. D.; Chen, C.-T. *J. Electrochem. Soc.* **1982**, *129*, 921.
(32) Odziemkowski, M. S.; Gillham, R. W. *Division of Environmental Chemistry, Extended Abstracts*; 213th American Chemical Society National Meeting, San Francisco, CA, 1997, Vol. 37, p 177.
(33) Schmuki, P.; Böhni, H. *Electrochim. Acta* **1995**, *40*, 775.
(34) Abrantes, L. M.; Peter, L. M. *J. Electroanal. Chem.* **1983**, *150*, 593.
(35) Stimming, U.; Schultze, J. W. *Ber. Bunsen-Ges. Phys. Chem.* **1976**, *80*, 1297.
(36) Wilhelm, S. M.; Yun, K. S.; Ballenger, L. W.; Hackerman, N. *J. Electrochem. Soc.* **1979**, *126*, 419.
(37) Schmuki, P.; Büchler, M.; Virtanen, S.; Böhni, H.; Muller, R.; Gauckler, L. J. *J. Electrochem. Soc.* **1995**, *142*, 3336.
(38) Searson, P. C.; Latanision, R. M.; Stimming, U. *J. Electrochem. Soc.* **1988**, *135*, 1358.
(39) Wilhelm, S. M.; Hackerman, N. *J. Electrochem. Soc.* **1981**, *128*, 1668.
(40) Kolthoff, I. M.; Lee, T. S.; Stocesova, D.; Parry, E. P. *Anal. Chem.* **1950**, *22*, 521.
(41) Finklea, H. O. In *Semiconductor Electrodes*; Finklea, H. O., Ed; Elsevier: New York, 1988; pp 1.
(42) Hummel, R. E. *Electronic Properties of Materials*, 2nd ed.; Springer-Verlag: New York, 1993.
(43) Benson, S. W. *Thermochemical Kinetics: Methods for the Estimation of Thermochemical Data and Rate Parameters*, 2nd ed.; Wiley: New York, 1976.
(44) Woodbury, G. *Physical Chemistry*; Brooks/Cole: Pacific Grove, CA, 1997.
(45) Vogel, T. M.; Criddle, C. S.; McCarty, P. L. *Environ. Sci. Technol.* **1987**, *21*, 722.
(46) Gerischer, H. In *Physical Chemistry: An Advanced Treatise*; Eyring, H., Ed; Academic: New York, 1970; Vol. IXA, p 463.
(47) Scherer, M. M.; Westall, J. C.; Ziomek-Moroz, M.; Tratnyek, P. G. *Environ. Sci. Technol.* **1997**, *31*, 2385.
(48) Stimming, U. *Electrochim. Acta* **1986**, *31*, 415.
(49) Schmickler, W. *Ber. Bunsen-Ges. Phys. Chem.* **1978**, *82*, 477.
(50) Schultze, J. W.; Stimming, U. *Z. Phys. Chem., Neue Folge* **1975**, *98*, 285.
(51) Meisterjahn, P.; Schultze, J. W.; Siemensmeyer, B.; Stimming, U.; Dean, M. H. *Chem. Phys.* **1990**, *141*, 131.
(52) Schreyer, A.; Eng, L.; Böhni, H. *J. Vac. Sci. Technol. B* **1996**, *14*, 1162.
(53) Gerischer, H. In *Photoelectrochemistry, Photocatalysis, and Photoreactors*; Schiavello, M., Ed; D. Reidel: Holland, 1985; p 39.
(54) Kieber, R. J.; Mopper, K. *Environ. Sci. Technol.* **1990**, *24*, 1477.
(55) Loraine, G. A. *Hazard. Waste Hazard. Mater.* **1993**, *10*, 185.
(56) Moore, J. H.; Davis, C. C.; Coplan, M. A. *Building Scientific Apparatus*; Addison-Wesley: Reading, MA, 1983.
(57) Cunningham, K. M.; Goldberg, M. C.; Weiner, E. R. *Environ. Sci. Technol.* **1988**, *22*, 1090.
(58) Langford, C. H.; Carey, J. H. *Can. J. Chem.* **1975**, *53*, 2430.
(59) Henglein, A.; Lindig, B.; Westerhausen, J. *J. Phys. Chem.* **1981**, *85*, 1627.
(60) Bahnemann, D. W.; Mönig, J.; Chapman, R. *J. Phys. Chem.* **1987**, *91*, 3782.
(61) Bard, A. J.; Faulkner, L. R. *Electrochemical Methods: Fundamentals and Applications*; Wiley: New York, 1980.
(62) Stumm, W. *Chemistry of the Solid-Water Interface: Processes at the Mineral-Water and Particle-Water Interface in Natural Systems*; Wiley: New York, 1992.
(63) Waite, T. D. In *Mineral-Water Interface Geochemistry*; Hochella, M. F., Jr.; White, A. F., Eds.; Mineralogical Society of America: Washington, DC, 1990; Vol. 23, p 559.
(64) Packer, J. E.; Wilson, R. L.; Bahnemann, D.; Asmus, K.-D. *J. Chem. Soc., Perkin Trans. 2* **1980**, 296.
(65) Huston, P. L.; Pignatello, J. J. *Environ. Sci. Technol.* **1996**, *30*, 3457.
(66) Schultze, J. W.; Danzfuss, B.; Meyer, O.; Stimming, U. *Mater. Sci. Eng.* **1985**, *69*, 273.
(67) Klausen, J.; Trober, S. P.; Haderlein, S. B.; Schwarzenbach, R. P. *Environ. Sci. Technol.* **1995**, *29*, 2396.
(68) Johnson, T. L.; Fish, W.; Gorby, Y. A.; Tratnyek, P. G. *J. Contam. Hydrol.* **1998**, *29*, 377.